Anal. Chem. **2005,** *77,* 5380−5384

Mathematical Model Describing Gradient Focusing Methods for Trace Analytes

Sandip Ghosal* and Jon Horek

Department of Mechanical Engineering, Northwestern University, 2145 Sheridan Road, Evanston, Illinois 60203

The problem of gradient focusing for concentrating trace analytes is considered. Variation of buffer viscosity, conductivity, and possibly also the ζ-potential results in a focusing point where the electrophoretic velocity is balanced by the electroosmotic flow (EOF) and where the sample concentrates. The axial inhomogeneity also results in an induced pressure gradient that alters the EOF profile and therefore causes Taylor dispersion. The coupled hydrodynamics and transport problem leading to the achievement of a steady state is studied in the context of the lubrication approximation: all variations in the axial direction take place over a length scale very much larger than the characteristic channel width. A single length scale σ_m and a single time scale τ is found to completely determine the dynamics of the evolution close to the focusing point. Using appropriate scaled variables, the time evolution of the concentration profile near equilibrium can be described by an inhomogeneous advection diffusion equation that is free of all parameters. Explicit formulas are deduced for the location of the peak centroid and its width as a function of time. A simple graphical method is proposed for optimizing the performance of the system when some tunable external parameters are available.

Historically, several methods have been developed for analyzing the components of a molecular mixture, among them various techniques utilizing chromatography and electrophoresis.[1] A common problem has been to improve the limit of detection, the lowest possible concentration at which an analyte is detected. This can be done either by improving the performance of the detector itself or by increasing the sample concentration prior to detection. Of these, the second appears more promising, because, for microfluidic capillaries, the optical path lengths involved are necessarily extremely short (20−40 μm) and detector technology is already pushed to its limit.

One way of preconcentrating the sample is to exploit some aspect of the underlying physics of transport to collect the analyte into a narrower region ("sample stacking"), thus increasing its maximum concentration.[2] In recent years, a body of experimental techniques known as gradient focusing methods has become popular for achieving this. For instance, it was recently demonstrated that temperature gradient focusing (TGF) can be used to increase sample concentration up to 10 000-fold during a 100-min interval.[3] In this technique, a temperature gradient is applied along a region of the microfluidic channel, and the resulting variation of fluid viscosity and conductivity alters both the electrophoretic mobility of the analytes and the bulk electroosmotic flow. At a certain point along the axis of the channel, the bulk flow and the electrophoretic velocity balance, leading the analyte to collect and concentrate in a narrow band. There also exist other experimental methods that create such gradients, for example, conductivity gradient focusing, electric field gradient focusing, and micellar affinity gradient focusing.[4−6]

FORMULATION

We consider a channel of arbitrary cross-sectional shape that does not vary in the axial (x) direction and one that is very long compared to its characteristic width. The channel contains a buffer for which the viscosity (μ), conductivity (σ), and wall ζ-potential (ζ) could vary in the axial direction: $\mu = \mu(x)$, $\sigma = \sigma(x)$, and $\zeta = \zeta(x)$, but do not depend on the cross-stream coordinates y and z. However, the characteristic length scale for any such variation is assumed large compared to the channel width. We assume further that the Debye length is very much smaller than the channel width such that the effect of the electric double layer at the wall can be adequately accounted for through the Helmholtz−Smoluchowski (HS) "slip" boundary conditions.[7] Finally, it is assumed that the molar concentration of analyte ions always remains far below that of the buffer ions so that nonlinearities arising out of the dependence of electrical conductivity on analyte concentration (electromigration dispersion) is entirely negligible.[8]

ELECTROOSMOTIC FLOW (EOF)

By virtue of our assumptions, the EOF in the channel may be treated using lubrication theory.[9] At lowest order, the flow is in the axial direction, and is composed of the HS electroosmotic component, as well as a component driven by the induced

* To whom correspondence should be addressed. E-mail: s-ghosal@northwestern.edu.

(1) Jorgenson, J., Phillips, M., Eds. *New Directions in Electrophoretic Methods*; American Chemical Society: Washington, DC, 1987.
(2) Chien, R. L. *Electrophoresis* **2003**, *24* (3), 486−497.
(3) Ross, D.; Locascio, L. E. *Anal. Chem.* **2002**, *74* (11), 2556−2564.
(4) Greenlee, R. D.; Ivory, C. F. *Biotechnol. Prog.* **1998**, *14* (2), 300−309.
(5) Koegler, W. S.; Ivory, C. F. *J. Chromatogr., A* **1996**, *726* (1−2), 229−236.
(6) Balss, K. M., et al. Micellar affinity gradient focusing: A new method for electrokinetic focusing. *J. Am. Chem. Soc.* **2004**, *126* (7), 1936−1937.
(7) Probstein, R. F. *Physicochemical Hydrodynamics An Introduction,* 2nd ed.; John Wiley & Sons: New York, 1994.
(8) Mikkers, F. E. P.; et al. *J. Chromatogr.* **1979**, *169*, 1−10.
(9) Batchelor, G. K. *An Introduction to Fluid Dynamics*; Cambridge University Press: Cambridge, U.K., 1967.

10.1021/ac050515e CCC: $30.25
Published on Web 07/12/2005

pressure gradient:[10]

$$u(x, y, z) = \frac{-p'(x)u_p(y, z)}{\mu(x)} - \frac{\epsilon\zeta(x)E(x)}{4\pi\mu(x)} \quad (1)$$

where ϵ is the dielectric constant of the fluid. The pressure $p(x)$ and axial electric field $E(x)$ depend only on the axial coordinate x in the lubrication limit. The function $u_p(y, z)$ is the solution of

$$\partial^2 u_p/\partial y^2 + \partial^2 u_p/\partial z^2 = -1 \quad (2)$$

subject to the Dirichlet condition

$$u_p|_\Gamma = 0 \quad (3)$$

where Γ is the bounding curve of the channel cross section. If the cross-sectional average is defined as $\bar{g} = A^{-1}\int\int g(y, z)\, dA$, and the axial average as $\langle h\rangle = L^{-1}\int_0^L h(x)\, dx$ (L is the channel length and A is the cross-sectional area), then if there is no pressure drop across the capillary, it follows, on integrating (1) over the entire volume of the fluid, that

$$\bar{u} = -(\epsilon\langle\zeta E\rangle/4\pi\langle\mu\rangle) \quad (4)$$

We define the function $F(x)$ as

$$F(x) = \sigma(0)\mu(0)/\sigma(x)\mu(x) \quad (5)$$

Since the current density, $J = \sigma E$, we can write the bulk flow (4) as

$$\bar{u} = \frac{-\epsilon\zeta_0 J}{4\pi\sigma_0\mu_0}\frac{\langle F\mu Z\rangle}{\langle\mu\rangle} = u_0\frac{\langle F\mu Z\rangle}{\langle\mu\rangle} \quad (6)$$

where $\sigma_0 = \sigma(0)$, $\mu_0 = \mu(0)$, $\zeta(0) = \zeta_0$, and $Z = \zeta/\zeta_0$. For convenience in our problem, we set the coordinate system such that the focusing point is at $x = 0$. Then

$$u_0 = -\epsilon\zeta_0 J/4\pi\sigma_0\mu_0 \quad (7)$$

is the HS slip velocity at the focusing point. Equation 6 is analogous to earlier results on flow in channels with variable wall ζ-potential.[11,10]

The electrophoretic velocity is proportional to $E(x)/\mu(x)$, so we can write it as

$$u_{ep}(x) = BJF(x) \quad (8)$$

where B is a constant. Since $F(0) = 1$, $u_{ep}(0) = BJ$ so that we have

$$u_{ep}(x) = u_{ep}(0)F(x) \quad (9)$$

AXIAL DISPERSION

1D Effective Equations. In the limit when all axial variations are on a length scale much larger than the channel width, we can employ the Taylor−Aris dispersion coefficients to describe axial diffusion; hence, the governing equation for the cross-sectionally averaged concentration is

$$\frac{\partial\bar{c}}{\partial t} + \frac{\partial(u_*(x)\bar{c})}{\partial x} = \frac{\partial}{\partial x}\left(D_*(x)\frac{\partial\bar{c}}{\partial x}\right) \quad (10)$$

Here $D_*(x) = D + D_T(x)$ is the effective diffusion coefficient, the sum of the molecular diffusion, and the Taylor dispersion and

$$u_*(x) = \bar{u} + u_{ep}(x) \quad (11)$$

is the net advective velocity.[12] For ease of notation, we will drop the overbar and denote the cross-sectionally average concentration simply as c.

Behavior Near the Focusing Point. We will assume that the peak is narrowly focused so that the variation of fluid properties over the width of a peak may be regarded as small. Since there is no net movement at the focusing point,

$$u_{ep}(0) = -\bar{u} \quad (12)$$

Taking the average over the cross section in (1) and solving the resulting equation for $p'(x)$, we obtain, after some simplification using (6) and (12),

$$\frac{p'(x)}{\mu(x)} = \frac{u_0}{\bar{u}_p}\left[F(x)Z(x) - \frac{\langle F\mu Z\rangle}{\langle\mu\rangle}\right] \quad (13)$$

Therefore, the full 3D pressure-driven (Poiseuille) component of the axial flow is

$$u_{poiss}(x, y, z) = -\frac{p'(x)}{\mu(x)}u_p(y, z) = u_0\frac{u_p(y, z)}{\bar{u}_p}\left[\frac{\langle F\mu Z\rangle}{\langle\mu\rangle} - F(x)Z(x)\right] \quad (14)$$

We can expand $F(x)$ in a Taylor series around the focusing point, $F(x) = F(0) + F'(0)x + \cdots$, and therefore write a linearized version of the net analyte velocity

$$u_*(x) = -\alpha x \quad (15)$$

where we define

$$\alpha = u_0(\langle F\mu Z\rangle/\langle\mu\rangle)F'(0) \quad (16)$$

We observe that the Taylor dispersion coefficient[13] may be written in general as

$$D_T(x) = A\phi\bar{u}_{poiss}{}^2(x)/D \quad (17)$$

where ϕ is a nondimensional geometric factor (e.g., for a circular

(10) Ghosal, S. *J. Fluid Mech.* **2002**, *459*, 103−128.
(11) Anderson, J. L.; Idol, W. K. *Chem. Eng. Commun.* **1985**, *38* (3), 93−106.
(12) Ghosal, S. *J. Fluid Mech.* **2003**, *491*, 285−300.
(13) Aris, R. *Proc. R. Soc. London, A* **1956**, *235* (1200), 67−77.

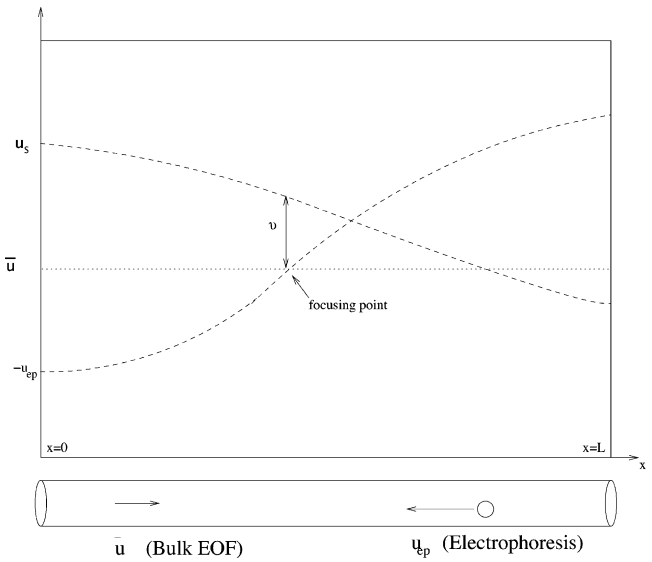

Figure 1. Simple geometrical method for calculating the focusing point and the dispersion coefficient.

cross section, $\phi = 1/48\pi$). On using (14), expanding $F(x)$ and $Z(x)$, and keeping only the leading term, we have

$$D_* = D + \frac{u_0^2 A\phi}{D}\left[\frac{\langle F\mu Z\rangle}{\langle\mu\rangle} - 1 + \cdots\right]^2 \approx D + \frac{A\phi}{D}v^2 \quad (18)$$

and

$$v = \bar{u} - u_0 = u_0\left[\frac{\langle F\mu Z\rangle}{\langle\mu\rangle} - 1\right] \quad (19)$$

The quantity v in eq 18 has a simple meaning. It is the difference between the bulk EOF speed and the HS slip velocity at the focusing point. Figure 1 shows a simple geometric way to calculate v. In Figure 1, the dashed lines show local values for the negative of the electrophoretic velocity, $-u_{ep}$, as well as the local HS slip velocity, u_s. The dotted horizontal line representing the bulk EOF speed is determined by the weighted average of the local HS slip velocity

$$\bar{u} = \frac{\langle\mu u_s\rangle}{\langle\mu\rangle} \quad (20)$$

The point where the dotted line and the dashed line representing $-u_{ep}$ intersect is then the focusing point. The vertical distance from this intersection to the line representing the local HS slip velocity u_s is the quantity v appearing in eq 18.

The behavior of the concentration distribution near the focusing point is therefore governed by

$$\frac{\partial c}{\partial t} - \alpha\frac{\partial}{\partial x}(xc) = D_*\frac{\partial^2 c}{\partial x^2} \quad (21)$$

with the constants α and D_* determined by eqs 16 and 18, respectively.

Time Evolution of Moments. The position of the peak and its variance may be determined from (21) using Aris's method of moments.[13] Let the kth moment of the distribution $c(x, t)$ be defined as

$$m_k(t) = \int_{-\infty}^{+\infty} c(x, t)x^k\,dx \quad (22)$$

therefore, multiplying eq 21 by x^k and integrating yields

$$\frac{dm_k}{dt} + k\alpha m_k = D_*\,k(k-1)m_{k-2} \quad (23)$$

In deriving (23), we have assumed that the peak is very far from the capillary inlet or outlet and that c and all its derivatives decay rapidly with increasing values of $|x|$, so that there are no contributions from the boundary terms arising from the integration by parts. Physically, these boundary conditions correspond to an analyte plug localized within a long channel. Other arrangements may be described by changing the boundary conditions. For example, if the channel is connected to relatively large capacity reservoirs at either end in which the analyte concentration remains practically constant at c_0, then the boundary conditions would be $c(0, t) = c(L, t) = c_0$ and the moment equations are augmented by contributions from boundary terms. Setting $k = 0, 1, 2$ in (23), the first three moment equations are

$$dm_0/dt = 0 \quad (24)$$

$$dm_1/dt = -\alpha m_1 \quad (25)$$

$$dm_2/dt + 2\alpha m_2 = 2D_* m_0 \quad (26)$$

The solutions are

$$m_0(t) = m_0(0) \quad (27)$$

$$m_1(t) = m_1(0)e^{-\alpha t} \quad (28)$$

$$m_2(t) = m_2(0)e^{-2\alpha t} + (D_* m_0/\alpha)(1 - e^{-2\alpha t}) \quad (29)$$

Therefore, the position of the peak centroid is

$$x_*(t) = m_1(t)/m_0 = x_*(0)e^{-\alpha t} \quad (30)$$

and the peak variance is

$$\sigma_*^2(t) = \frac{m_2(t)}{m_0} - \left(\frac{m_1(t)}{m_0}\right)^2 = \sigma_*^2(0)e^{-2\alpha t} + \frac{D_*}{\alpha}(1 - e^{-2\alpha t}) \quad (31)$$

Equilibrium Profile. Equation 21 admits a unique steady-state solution, provided that c and $c'(x)$ are required to vanish sufficiently rapidly at $x \to \pm\infty$. At steady state,

$$-\alpha\frac{d}{dx}(xc) = D_*\frac{d^2 c}{dx^2} \quad (32)$$

which is readily integrated to yield the equilibrium profile,

$$c_{eq}(x) = c_{eq}(0)\ \exp[-\alpha x^2/2D_*] \tag{33}$$

Thus, the steady state is a Gaussian with variance

$$\sigma_m{}^2 \equiv \sigma_*{}^2(\infty) = D_*/\alpha \tag{34}$$

as observed by Ross and Locascio.[3] The value of $c_{eq}(0)$ can be found from the requirement

$$A\int_{-\infty}^{\infty} c_{eq}(x)\ dx = N \tag{35}$$

where N is the number of moles (if c is expressed as moles/volume) of analyte present. Thus,

$$c_{eq}(0) = N/A\sigma_m\sqrt{2\pi} \tag{36}$$

TIME EVOLUTION OF CONCENTRATION PROFILES

Let us rewrite eq 21 in terms of the dimensionless variables $X = x/L_*$, $T = t/\tau$, and $C = c/c_*$, where L_*, τ, and c_* are suitable reference values for length, time, and concentration. In particular, selecting $L_* = \sigma_m = (D_*/\alpha)^{1/2}$, and $\tau = \alpha^{-1}$ and $c_* = c_{eq}(0)$ yields

$$\frac{\partial C}{\partial T} = \frac{\partial}{\partial X}(XC) + \frac{\partial^2 C}{\partial X^2} \tag{37}$$

The equilibrium profile is

$$C(X,\infty) = e^{-X^2/2} \tag{38}$$

In terms of these scaled variables, eq 37 is free of all parameters. It only depends on the initial profile $C(X, 0)$, which can be any smooth function that satisfies the requirement imposed by mass conservation:

$$\int_{-\infty}^{\infty} C(X, 0)\ dX = \int_{-\infty}^{\infty} C(X,\infty)\ dX = \sqrt{2\pi} \tag{39}$$

Equation 37 was solved numerically using a computational scheme that used second-order central differencing in space coupled to a fourth-order Runge−Kutta predictor−corrector scheme for time. The initial condition was chosen quite arbitrarily as a "quasi" rectangular initial profile (i.e., a rectangle with slightly rounded corners to avoid resolution difficulties with the numerical scheme). The curves in Figure 2 show snapshots of the concentration profile $C(X, T)$ once every 1250 units of the variable time, T.

SUMMARY

Gradient focusing is an effective method for trace analyte separation and detection. A mathematical model describing the time-dependent problem of the evolution of the analyte concentration profile to the final steady state is addressed. The model takes into account the fact that the axial inhomogeneity created by the variation of the focusing parameters along the channel would create an induced pressure gradient and associated Taylor dispersion. The time scale $\tau = \alpha^{-1}$ and length scale σ_m fully characterizes the problem in the neighborhood of the focusing point. The peak approaches the focus point and the variance $\sigma_*(t)$ approaches the minimum variance exponentially with a time constant $\sim\tau$. Using σ_m and τ as length and time scales, the evolution of the concentration may be described by eq 37, which is free of all parameters. At steady state, it describes a Gaussian profile.

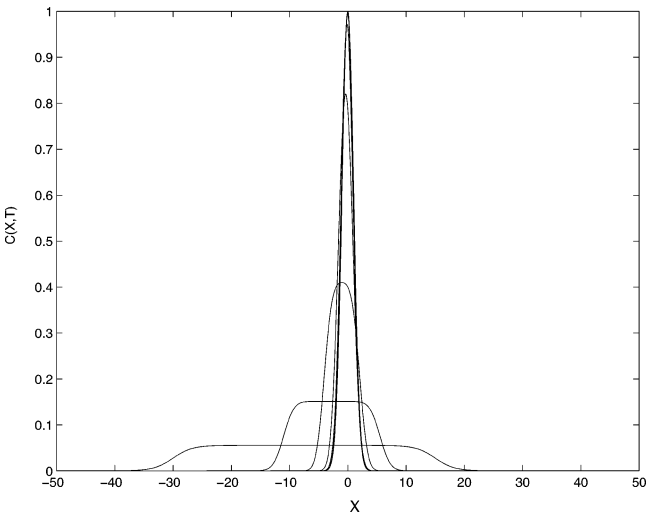

Figure 2. Evolution of the dimensionless concentration $C(X, T)$. Curves are separated by time intervals $\Delta T = 1250$ units.

The assumption of "slow axial variations" on which the theoretical developments above are based will now be made more precise. The important characteristic length scales in this problem are a_0, a typical channel width, $L_f = u_0/\alpha$, which from eq 16 is a characteristic distance over which the focusing parameters vary. In order that the lubrication theory be applicable, we must have $L_f \gg a_0$. For the use of the Taylor−Aris effective diffusion coefficients to be justified, the concentration profile must vary "slowly", which means $\sigma_m \gg a_0$. However, at the same time, for the linearization leading to eq 15 to be valid, we must have $\sigma_m \ll L_f$. All of these relations may be written together in the form

$$L_f \gg \sigma_m \gg a_0 \tag{40}$$

The quantity σ_m may be expressed in terms of the Péclet number $Pe = a_0u_0/D$ using eqs 34 and 18:

$$\sigma_m = \sqrt{\frac{D_*}{\alpha}} = \sqrt{\frac{L_fD(1 + cPe^2)}{u_0}} = \sqrt{\frac{L_fa_0(1 + cPe^2)}{Pe}} \tag{41}$$

where c is a dimensionless constant of order unity. If $Pe \ll 1$, then the right-hand side of eq 41 reduces to $(L_fa_0/Pe)^{1/2}$. If $Pe \gg 1$, then the right-hand side reduces to $(cL_fa_0Pe)^{1/2}$. The inequality 40 could therefore be written as

$$L_f \gg \max(Pe,Pe^{-1})a_0 \tag{42}$$

where "max" denotes the larger of the two; that is, Pe if $Pe > 1$ and Pe^{-1} otherwise. In the applications, we are concerned with

$Pe \sim 100$ or higher. Therefore, the requirement of slow variations may be interpreted as $L_f \gg a_0 Pe$.

The simple model discussed here can be used to understand some general features of gradient focusing systems and how they might be optimized for performance. Clearly, from (34), one would want to make α as large as possible; that is, $F'(0)$ should be large. This on the other hand would imply large variations in F and, therefore, generally speaking larger values of D_*. Thus, the beneficial effects of large gradients is partially offset by the fact that the resultant axial variations add to the Taylor dispersion. Figure 1 suggests a way of optimizing the design of a gradient focusing system in situations where it is technically possible to control the shapes of the curves u_s, u_{ep}, or both to some degree. This could be the case, for example in TGF with multiple heating elements along the axis that enables a piecewise linear temperature profile to be established along the channel. If the available parameters are adjusted in such a manner that the curves for u_s, $\bar{u}$, and $-u_{ep}$ intersect at a single point or as close to a single point as possible, then v and therefore the Taylor dispersion is minimized. In this way, the present analysis could be used to calculate such design parameters as the optimum placement of a heating element along the channel.

ACKNOWLEDGMENT

Support from the NSF under Grant CTS-0330604 (S.G.) and under the Graduate Research Fellowship Program (J.H.) is gratefully acknowledged.

Received for review March 26, 2005. Accepted June 15, 2005.

AC050515E